Rapid #: -15753688

CROSS REF ID: **901947**

LENDER: **VTU :: Main Library**

BORROWER: **WVU :: Downtown Campus Library**

TYPE:	Article CC:CCG
JOURNAL TITLE:	Astrobiology (Larchmont, N.Y. Online)
USER JOURNAL TITLE:	Astrobiology
ARTICLE TITLE:	Lipid Biomarkers in Ephemeral Acid Salt Lake Mudflat/Sandflat Sediments: Implications for Mars.
ARTICLE AUTHOR:	Johnson, Sarah Stewart
VOLUME:	20
ISSUE:	2
MONTH:	02
YEAR:	2020
PAGES:	167-178
ISSN:	1557-8070
OCLC #:	

Processed by RapidX: 2/10/2020 7:30:29 AM

ASTROBIOLOGY
Volume 20, Number 2, 2020

DOI: 10.1089/ast.2017.1812

Lipid Biomarkers in Ephemeral Acid Salt Lake Mudflat/Sandflat Sediments: Implications for Mars

Sarah Stewart Johnson,[1,2] Maëva Millan,[1,3] Heather Graham,[3] Kathleen C. Benison,[4] Amy J. Williams,[5] Amy McAdam,[3] Christine A. Knudson,[3,6] Slavka Andrejkovičová,[3,6] and Cherie Achilles[3]

Abstract

Sedimentary strata on Mars often contain a mix of sulfates, iron oxides, chlorides, and phyllosilicates, a mineral assemblage that is unique on Earth to acid brine environments. To help characterize the astrobiological potential of depositional environments with similar minerals present, samples from four naturally occurring acidic salt lakes and adjacent mudflats/sandflats in the vicinity of Norseman, Western Australia, were collected and analyzed. Lipid biomarkers were extracted and quantified, revealing biomarkers from vascular plants alongside trace microbial lipids. The resilience of lipids from dead organic material in these acid saline sediments through the pervasive stages of early diagenesis lends support to the idea that sulfates, in tandem with phyllosilicates and iron oxides, could be a viable target for biomarkers on Mars. To fully understand the astrobiological potential of these depositional environments, additional investigations of organic preservation in ancient acidic saline sedimentary environments are needed. Key Words: Astrobiology—Mars—Acid salt lakes—Lipid biomarkers—Biosignatures—Lakes. Astrobiology 20, 167–178.

1. Introduction

Although abiotic synthesis of some organic compounds may occur in hydrothermal settings (McCollom and Seewald, 2007), the vast majority of sedimentary organic matter reflects biological processes that are highly characteristic of the depositional environment. Biomarkers—organic compounds derived from living organisms—are particularly important in reconstructing Earth's microbial history before the Cambrian radiation emergence of readily fossilized body features (Simoneit *et al.*, 1998). Biomarkers have been found in rocks and sediments that are associated with some of the earliest life forms on Earth, and they have been used to characterize both physical environments and primitive biological systems (see examples in Peters *et al.*, 2007). Lipid biomarkers, in particular, are paramount in the identification of ancient bacterial metabolism that is preserved in Archaean and Proterozoic rocks (Summons and Walter, 1990), as well as in modern microbial communities (White, 1983). Microbial lipids that survive in the rock record typically have highly branched or cyclic hydrocarbons, such as isoprenoids and sterols, which are resistant to the early stages of diagenesis, during which time most degradation occurs. Often, the more polar membrane lipids such as fatty acids are rapidly degraded (De Leeuw and Largeau, 1993), although recent research demonstrates that select taphonomic windows exist that allow phospho- and glycolipids to survive initial diagenesis (Wilhelm *et al.*, 2017, 2018).

If similar biomarkers formed and were preserved in the geological record on the surface of Mars, where would we be most likely to find them? The best way to answer this might be to evaluate biomarker preservation in analog mineral environments on Earth. In the vicinity of Norseman, Western Australia are dozens of acid salt lakes hosted by the deeply weathered Archaean rocks of the Yilgarn Craton (see Fig. 1). They range in diameter from m^2 to km^2, and they are marked by cycles of flooding, evapoconcentration, and desiccation (Benison *et al.*, 2007), as well as by winds. Despite the extreme conditions (pHs as low as 1, salinity as high as 32% total dissolved solids, high fluxes of solar radiation, water

[1]Department of Biology, Georgetown University, Washington, District of Columbia.
[2]Program on Science, Technology, and International Affairs, Georgetown University, Washington, District of Columbia.
[3]NASA Goddard Space Flight Center, Greenbelt, Maryland.
[4]Department of Geology and Geography, West Virginia University, Morgantown, West Virginia.
[5]Department of Geological Sciences, University of Florida, Gainesville, Florida.
[6]Center for Research and Exploration in Space Sciences and Technology/University of Maryland College Park, College Park, Maryland.

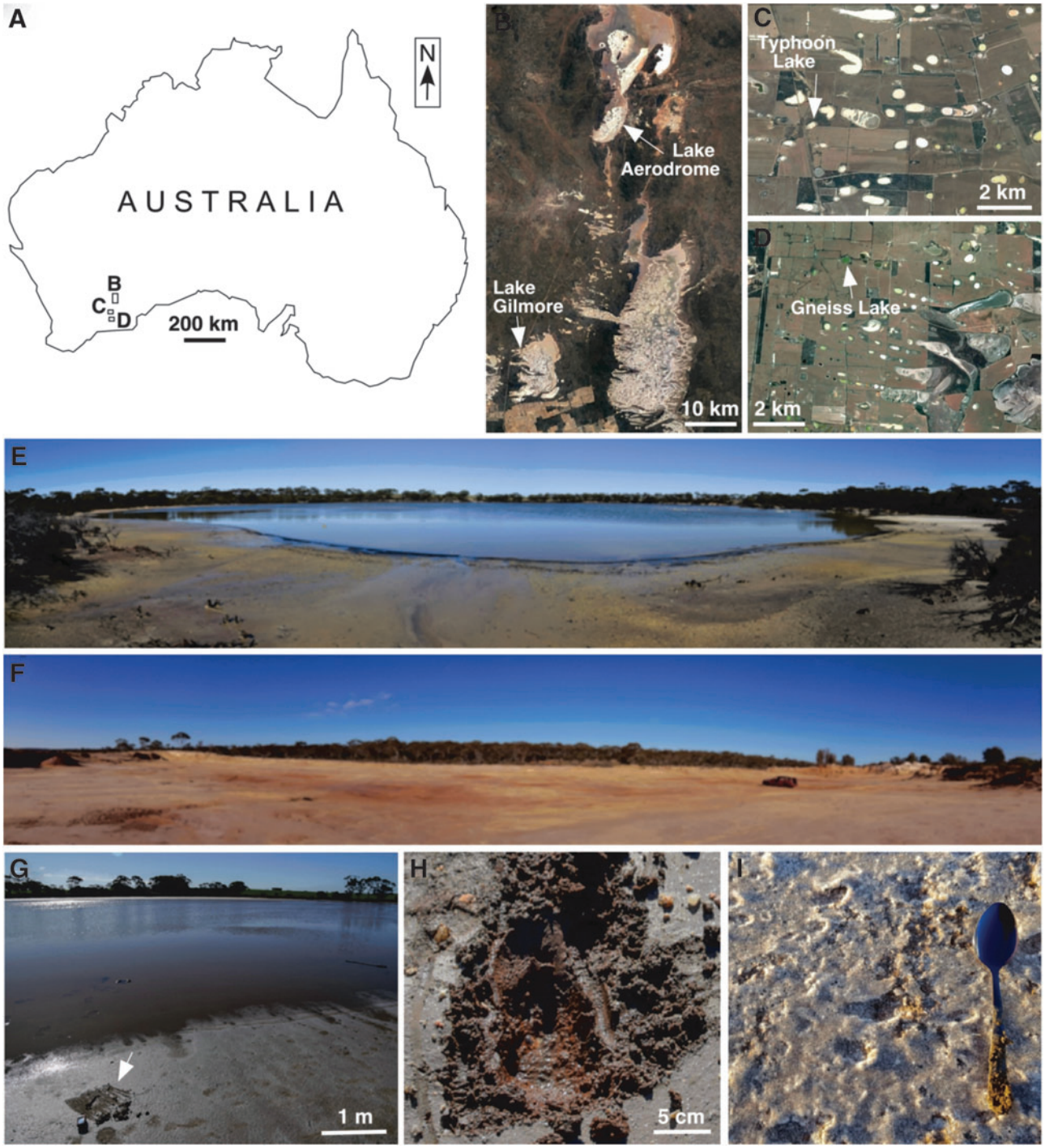

FIG. 1. Sampling sites at ephemeral acid saline lakes in southern Western Australia. **(A)** Map of Australia showing approximate locations of sampling sites. **(B–D)** Satellite images of lakes, courtesy of Google Earth and Landsat/Copernicus. Each satellite image is keyed to location on the map of Australia to the left. **(E)** Photo of Gneiss Lake at flooding stage and surrounding acid saline mud/sandflat with yellow and brown sediments. **(F)** Photo of Lake Aerodrome at desiccation stage. Red car on right for scale. **(G)** Lake Typhoon at flooding stage. Arrow points to sampling site on acid saline mud/sandflat, 1 m from lake shore. **(H)** Bedding plane view of sampling site at Lake Gneiss mud/sandflat. **(I)** Bedding plane view of sampling site at desiccated Lake Gilmore. Spoon for scale. Lake names are taken from Benison *et al.* (2007) and Bowen and Benison (2009).

stress during desiccation, high metal concentrations, and large shifts in diurnal temperature), these sites are highly habitable, and they are home to a diverse bacterial-, archaeal-, algal-, and fungal-rich microbiome (Mormile *et al.*, 2009; Johnson *et al.*, 2015; Zaikova *et al.*, 2018; Aerts *et al.*, 2019).

The acid brine lakes and associated mudflats/sandflats have been interpreted as an excellent analogue for martian sedimentary deposits for three reasons (Benison and LaClair, 2003; Benison and Bowen, 2006). First, there are similar sedimentary textures and sedimentary structures, including

laminations, wave ripple cross-bedding, and mudcracks in both terrestrial and martian environments, suggesting processes such as flooding, desiccation, and eolian reworking. Second, there are similar diagenetic features, including iron oxide concretions, displacive crystals, and sulfate veins, likely formed from acid saline groundwaters. Third and most importantly, the sedimentary mineral assemblage on Mars is quite similar to that of acid saline lakes in Western Australia.

The mineral assemblage at acid saline lakes and mudflats/sandflats in southern Western Australia is unusual and includes a siliciclastic component, chlorides, sulfates, iron oxides, phyllosilicates, and opaline silica (Benison *et al.*, 2007; Story *et al.*, 2010).

Halite, gypsum (and other sulfates such as epsomite and basanite), hematite, kaolinite, and, less commonly, jarosite, alunite, and silica precipitate directly from acid saline lakes as chemical sediments (Benison *et al.*, 2007). Halite and gypsum also grow from acid saline groundwater centimeters below the surface of mudflats and sandflats adjacent to the lakes, making displacive halite and gypsum, as well as halite and gypsum intergranular cements (Bowen *et al.*, 2013). Hematite, jarosite, alunite, and kaolinite also precipitate directly from acid saline groundwaters as early intergranular cements (Benison *et al.*, 2007: Bowen *et al.*, 2012). Hematite concretions form early in Western Australian acid saline lake and mudflat/sandflat sediments and contain hematite, jarosite, gypsum, halite, and kaolinite (Bowen *et al.*, 2008). The siliciclastic component of the sediments includes quartz and feldspar sand and mud grains that are the products of the weathering of Archaean host rocks (Bowen *et al.*, 2013).

Some of these minerals on Mars, particularly jarosite and alunite, serve as strong indicators of past acidic conditions. Jarosite, a hydrated iron sulfate that forms in acid saline waters (Nordstrom, 1982; Klingelhöfer *et al.*, 2004), was first hypothesized on Mars by Burns (1987), then discovered by the Opportunity rover in 2004 (Klingelhöfer *et al.*, 2004), suggesting that acidic conditions once dominated the landscape at Meridiani Planum. Jarosite has since been detected in other multiple sites on Mars, suggesting that it is a relatively common mineral (Cull *et al.*, 2014; Léveillé *et al.*, 2015). Alunite, a hydrated aluminum sulfate in the same family as jarosite, has been found in the Terra Sirenum region of Mars, within a spatially extensive formation within Cross crater, where in some areas it is closely associated with kaolinite. Alunite also strongly suggests low pH, sulfuric fluids at or near the martian surface (Ehlmann *et al.*, 2016).

Oxidized minerals have long been considered weak targets for the preservation of organic molecules (Klein, 2005). Thermodynamics suggest that organics will quickly react with SO^{2-} and Fe^{3+} (Sumner, 2004; Stumm and Morgan, 2012). The kinetics of organic carbon oxidation in the presence of iron is believed to be extremely rapid—months to years under most conditions—largely due to the generation of free radicals and H_2O_2 on the surface of iron-bearing minerals, and the calculations of Stumm and Morgan (1996) suggest that Fe(III)-bearing minerals are not stable at the low electron potentials that are necessary for organic carbon stability (Sumner, 2004; Stumm and Morgan, 2012). Sulfate reduction in the presence of organics, while slower in general, requires the transfer of more electrons and is believed to occur at a faster rate at low pH conditions (Ohmoto and Lasaga, 1982).

Mineral stability fields, however, depend critically on ion pairing in solution. This, in turn, depends on brine compositions and pH. Although significant progress has been made in this area—on how Mg, Ca, and Fe-sulfates might have formed from the evaporation of acidic fluids derived from weathering olivine-bearing basalt (Tosca *et al.*, 2005), on how iron-bearing phyllosilicates might have formed from weathering and hydrothermal alteration of martian basalt (Catalano, 2013), and on how clay-bearing sequences might have formed through downward percolation and neutralization of acidic H_2SO_4–HCl solutions (Zolotov and Mironenko, 2016)—these compositions are not fully constrained for the early martian surface.

To analyze the astrobiological potential of mixtures of sulfates, iron oxides, and phyllosilicates in a highly acidic and saline terrestrial Mars analogue, this study investigated the types of biomarkers present and the range of biomarker recovery by using gas chromatography-mass spectrometry (GC-MS), which illuminates the chemical structure of biomolecules from characteristic fragment ions in their mass spectra.

2. Materials and Methods

2.1. Sample acquisition

Sediment samples were collected in June 2018 from four acid saline lakes within the vicinity of Norseman in southern Western Australia. The ambient air temperatures were high (up to 34.6°C). Lakes in the region are ephemeral; of those with standing surface water in June 2018, lake diameters were typically less than a few 100 m and no more than a meter deep. Lakes Aerodrome, Gilmore, Gneiss, and Typhoon were chosen because they had been previously studied as part of an initial biomarker study (Johnson, 2008) and had long records of geological and geochemical observation (*e.g.*, Benison and LaClair, 2003; Benison and Bowen, 2006, 2015; Benison *et al.*, 2007, 2008; Bowen and Benison, 2009; Story *et al.*, 2010; Bowen *et al.*, 2012, 2013; Johnson *et al.*, 2015).

Sediment samples were collected from acid saline mudflats/sandflats $\sim$1 m from the active shoreline of flooded Lake Gneiss and Typhoon Lake. Other samples were collected from the lake facies of desiccated Lake Aerodrome and Lake Gilmore. At these sites, minerals and water chemistry change through time. At the time of sampling, Lake Gneiss was underlain by yellowish-brown mud and a thin halite layer of $\sim$1 mm in thickness. The nearby Typhoon Lake had a thicker halite layer, $\sim$3 mm in thickness; Lake Aerodrome, near an unpaved landing strip on the southern part of Cowan Basin, is composed of a bed of bottom-growth gypsum crystals up to 5 cm in length. At Lake Gilmore, the salt crust was much more prevalent, $\sim$1 cm in thickness.

Sampling in the field and subsequent laboratory procedures were conducted with sterile procedures to avoid contamination. At each sampling site, samples of $\sim$100-g wet weight were collected with organically clean spatulas and organically clean glass jars (precombusted at 550°C for 8 h) from just beneath the salt crust to a depth of $\sim$5 cm (Table 1). Samples were kept frozen until the time of analysis. Approximately 10 g of material was subsampled for

Table 1. Environmental Characteristics for the Four Mud/Sandflats Sampled in this Study

Sample Name	*South Latitude*	*East Longitude*	*Site Characteristics*	*pH/TDS*	*pH Range Previously Observed*	C (*μMol/g*)	N (*μMol/g*)
Aerodrome	32.211	121.759	Light brown/yellow mud/ sandflat from beneath a thin (~3–5 mm) halite crust	Dry	2.7–4.5	74.4	Below Detection
Gilmore	32.610	121.561	Red/orange mud/sandflat beneath a thin (~2–3 mm) halite crust	Dry	2.6–5.8	650.3	49.9
Gneiss	33.220	121.755	Brown/red subaerial mud/sandflat ~1 m from shoreline, no salt crust Gray subaerial mud/sandflat	2.1/250 ‰	1.4–3.7	321.4	20.9
Typhoon	33.075	121.685	~1 m from shoreline, beneath a very thin (~1 mm) halite crust	2.7/280 ‰	3.2–4.2	297.4	29.8

If present, pH and TDS were also measured on lake water. Previously observed pH data are from the supplementary information in Bowen and Benison (2009).
TDS, total dissolved solids.

mineralogical and particulate organic carbon and nitrogen analyses. The other 90 g was reserved for lipid extraction. For the sample sites where lake water was present, a water sample was also collected in a sterile 50-mL falcon tube.

2.2. X-ray diffraction

Samples were crushed via mortar and pestle and sieved to <63 μm for powder X-ray diffraction (XRD) analyses on a Bruker D8 Discover diffractometer. The patterns were acquired from 2 to 70° 2θ (Cu Kα radiation, $\lambda = 1.54059$ Å), and quantitative mineralogy was obtained by Rietveld refinement methods using the MDI (Materials Data Incorporated) Jade analysis software. Due to the poorly crystalline nature of certain phyllosilicate minerals (*e.g.*, kaolinite, smectite), standard Rietveld refinement methods cannot be used to properly quantify the abundance of such phases. Among the samples analyzed, kaolinite was identified by its characteristic ~7.2 Å peak and quantified by combining a whole pattern fitting technique with the Rietveld refinement of the crystalline fraction. The scale factor of a pure kaolinite pattern (Clay Mineral Society KGa-2; relative intensity ratio = 2.1) was optimized to yield an abundance relative to the crystalline phases. As will be discussed later in Section 3, the sample diffraction patterns show lower 001:02*l* kaolinite intensity ratios than expected for randomized patterns, indicative of acid alteration of the kaolinite (Pentrak *et al.*, 2012). To minimize quantification uncertainties due to kaolinite alteration, the kaolinite abundance was estimated from 02*l* band scattering, a more stable measurement region compared with the 001 basal peak. Clay minerals were characterized by isolating the <2-μm size fraction and performing XRD on oriented mounts.

2.3. Contextual environmental measurements

For lakes where water was present, the water was analyzed for pH on return to the lab with a Mettler Toledo pH meter. Total dissolved solids were measured with VeeGee STX-3 handheld refractometer at 1:10 dilution with deionized water. Particulate organic carbon and nitrogen on all four mudflat/sandflat samples were measured according to standard protocols by using a CHN Elemental Analyzer at Woods Hole Oceanographic Institution Nutrient Analytical Facility, Massachusetts (Table 1).

2.4. Lipid extraction

Sediment samples of ~90-g wet weight (mixtures of sand, mud, salt crystals, and groundwater) were freeze dried for 36 h. The samples were then crushed to a fine powder by using a solvent-washed (3× methanol, 3× methanol: dichloromethane 1:1, 3× dichloromethane) mortar and pestle. Lipids were extracted by using a modified Bligh and Dyer method (Bligh and Dyer, 1959) alongside an extraction blank to monitor for any signs of contamination. Extractions took place in prewashed 50-mL Teflon tubes that were ultracleaned by two sequential 30-min sonications in methanol and dichloromethane. Nineteen milliliters of a 10:5:4 mixture of methanol: chloroform: dichloromethane-washed H_2O was added to each dry sample powder (of approximate weight 10 g) within the Teflon tubes. A mixture containing four internal standards—heneicosane (C_{21}), 2-methyloctadecanoic acid, 1-nonadecanol (C_{19}) and p-terphenyl-d_{14}—was then added to the total lipid extract (TLE).

The sample tubes were then vortexed for 5 min and sonicated for 20 min before centrifugation at 2500 rpm for 10 min. The liquid phase was transferred to a precombusted glass separatory funnel, and the process was repeated three times with the remaining sediment. For the final extraction, 19 mL of a 10:5:4 mixture of methanol: dichloromethane: H_2O with 1% trichloroacetic acid was used; then, 30 mL of deionized water was added to the separatory funnel to aid in phase separation. The aqueous phase was re-extracted two more times by using dichloromethane.

To desulfurize samples, acid-activated and solvent-cleaned copper pellets were added to the 60-mL precombusted glass vial containing the TLE before drying it and allowed to sit overnight. The TLE was reduced to less than 50 μL under N_2 gas.

2.5. Silica gel column separation

Approximately half of the total lipid extract was then applied to a 10-cm silica gel pipet column for each sample. Columns with each sample, alongside an extraction blank to monitor for signs of contamination, were sequentially eluted with 1.4 column-volumes of hexane and 2 column volumes of 8:2 hexane-dichloromethane to obtain the nonpolar fractions F1 and F2; this was followed by 2 column volumes of dichloromethane for fraction F3, 2 column volumes of 8:2 dichloromethane-ethyl acetate for fraction F4, and 3 column volumes of 7:3 dichloromethane-methanol for fraction F5. Each fraction was then gently evaporated under N_2 gas. Because of an issue with clumping of the silica gel, the column fractions were lost for the Lake Gilmore mudflat/sandflat sample (for this reason, only the total lipid extract was analyzed on the GC-MS and only those results are reported in Table 2; for all other samples, results from the better separated fractions are reported in Table 2).

2.6. Derivatization for GC-MS

Trimethylsilyl (TMS) reagents were used to derivatize (reducing the polarity of) functional groups in polar fractions F3, F4, and F5 before GC-MS analysis. Nonpolar fractions were reconstituted in 20 μL of hexanes. Ten microliters of bis(trimethylsilyl)trifluoroacetamide (BSTFA) in 10 μL of pyridine was added; then, samples were heated at 70°C for 30 min for the derivatization to occur. All polar fractions were run on the GC-MS within 36 h of derivatization.

2.7. GC-MS conditions

An injection volume of 1 μL from each fraction was analyzed on a ThermoFisher Trace 1310 gas chromatograph coupled to a ISQ-LT quadrupole mass-spectrometer (GC-MS). The GC is equipped with a programmed-temperature vaporization (PTV) inlet, a 30-m MXT-5 capillary column with 0.25-mm i.d., and 0.25-m film thickness; helium (purity ≥99.999%) was used as carrier gas. The PTV injector temperature was set at 330°C to prevent any condensation of the compounds analyzed. Injections were administered in split mode with a 5-mL/min split flow and a 1.2-mL/min constant carrier flow rate. The five fractions were analyzed by using the same GC temperature program: initial temperature of 60°C immediately followed by a 10°C/min ramp to 150°C, immediately followed by a second ramp temperature at 4°C/min to 350°C held for 10 min. This temperature program allowed all the compounds targeted to be analyzed while being well separated.

Both the MS transfer line and ion source temperatures were set at 300°C. The MS was set to scan the ions produced from the electron impact ionization source (70 eV) in the range m/z 30 to 600. A solvent delay of 6 min was applied to preserve the MS filament and prevent saturation of the GC column by the solvents associated with the fractions and the BSTFA derivatization reagent.

2.8. Peak identifications

Chromatograms and the mass spectra for different compounds were viewed by using the Xcalibur qual browser software from ThermoFisher. Identifications were based on spectral reduction by AMDIS software followed by NIST Spectral Library software matches when available. Otherwise, spectra were identified by comparison with a laboratory-acquired spectral library and retention times of known molecules.

3. Mineralogy Results

Mineralogical composition derived from XRD analyses of the samples is shown in Fig. 2. Quartz, halite, and kaolinite were present in all samples. Quartz was the dominant mineral in Aerodrome (93.5 wt.%), Typhoon (85.8 wt.%), and Gilmore samples (39.7 wt.%). Halite content varies between 2.4 (Aerodrome) and ~16 wt.% (Gilmore and Gneiss).

Aerodrome and Typhoon, both quartz rich samples, contained very low amounts of kaolinite (0.8–1 wt.%) compared with Gilmore and Gneiss (7.7–10.6 wt.%). Kaolinite exhibited a striking decrease in d_{001} peak intensity at 12.2° 2Θ compared with that expected from kaolinite (Fig. 2). This preferential decrease in d_{001} peak intensity compared with d_{021} peak intensity (20° 2Θ) is a characteristic of acid attack (Pentrák *et al.*, 2012). XRD analyses of oriented mounts of the <2-μm size fraction of each sample (not reported) confirmed the presence of kaolinite in each sample and also revealed the presence of a trace 10 Å phyllosilicate that could be either illite or a mica mineral.

Plagioclase is identified in most samples (1.7–6.6 wt.%) as well as alunite, which is most abundant (49.5 wt.%) in the sample from the most acidic lake Gneiss (pH = 1, Table 1). Gilmore is the only sample containing gypsum with a significant abundance of 29 wt.%. Hematite and goethite were identified as minor phases in Aerodrome and Gneiss with 0.6 and 1.8 wt.%, respectively. It is important to note, however, that mineral suites in the Western Australian acid saline lakes and adjacent mudflats/sandflats are heterogeneous over meter-scales and change in mineral relative abundances in response to flooding, evapoconcentration, desiccation, and host rock composition (Benison *et al.*, 2007; Story *et al.*, 2010; Bowen *et al.*, 2012).

4. Lipid Results

Typical GC-MS chromatograms show the most abundant lipids recovered from the Bligh and Dyer-extracted nonpolar fractions (F1 and F2) and polar (F3, F4, and F5) fractions. Representative chromatograms are presented in Figs. 3–5. Identifications are noted in Table 2. The following internal standards were used: heneicosane (C_{21}), 2-methyloctadecanoic acid, 1-nonadecanol (C_{19}), and p-terphenyl-d_{14}.

n-Alkanes were identified in fractions F1 and F2 after Bligh–Dyer extractions and column separation. The *n*-alkanes range in carbon number from 17 to 35, whereas the most dominant homologues are the C_{25}–C_{31} *n*-alkanes; no evidence of cyanobacteria in short chain *n*-alkanes was seen. There is a strong odd over even carbon number predominance (Fig. 3).

Fatty acids in the polar fractions range in carbon number from 12 to 32 and *n*-alcohols range from 14 to 32. Even numbered carbon compounds dominate the distributions of fatty acids and *n*-alcohols (Fig. 4). Only very low levels of branched fatty acids were detected (C15:1, C16:1, and C18:1, all <1% of the total fatty acid distribution). Sterols, ursolic acid derivatives, and betulin were also found in high levels in the polar fractions (Fig. 5). Based on retention

TABLE 2. DETECTIONS SHOWN AS PERCENTAGES OF TOTAL ALKANES, FATTY ACIDS, ALCOHOLS, AND STEROLS IN EACH SAMPLE

Alkanes

Fraction	Sample	C17	C18	C19	C20	C21	C22	C23	C24	C25	C26	C27	C28	C29	C30	C31	C32	C33	C34	C35
F1	Aerodrome	0.0	0.1	0.4	1.0	12.6	3.1	6.5	4.0	9.8	4.8	14.3	4.0	18.2	1.5	13.5	0.6	5.2	0.2	0.2
	Gilmore (TLE)	3.0	0.6	1.3	1.8	4.6	2.8	6.1	2.5	7.7	2.9	9.8	2.5	18.6	2.1	20.4	1.2	10.9	0.6	0.7
	Gneiss		0.3	1.1	2.0	21.2	3.6	6.1	4.1	11.1	3.3	10.9	2.5	13.1	1.0	13.4	0.7	4.4	0.4	0.9
	Typhoon	0.2	0.5	2.1	3.6	8.9	5.5	8.5	5.2	10.6	5.5	12.8	4.4	13.4	1.8	10.3	0.7	5.6	0.2	0.4
F2	Aerodrome		0.4	1.2	1.3	17.7	5.6	3.7	2.4	5.8	3.2	10.5	3.4	13.4	2.9	17.9	1.2	7.4	1.6	0.6
	Gilmore (TLE)	3.0	0.6	1.3	1.8	4.6	2.8	6.1	2.5	7.7	2.9	9.8	2.5	18.6	2.1	20.4	1.2	10.9	0.6	0.7
	Gneiss	0.3	0.7	3.1	2.5	18.5	5.1	5.4	4.0	9.4	4.2	10.1	4.0	10.2	2.2	12.1	0.9	5.1	1.3	0.9
	Typhoon	0.3	0.5	2.0	2.2	6.4	4.4	7.1	4.2	12.5	6.4	14.0	4.0	15.4	1.7	11.7	0.8	5.7	0.4	0.3

Fatty Acids

Fraction	Sample	C12	C13	C14	C15	C16	C17	C18	C19	C20	C21	C22	C23	C24	C25	C26	C27	C28	C29	C30	C31	C32
F3	Aerodrome					59.5	1.2	39.2														
	Gilmore (TLE)	0.6		2.7	0.8	28.6	1.1	10.6	1.1	5.2	0.5	4.5	14.8	5.6	17.9	6.1						
	Gneiss					59.5	1.5	39.0														
	Typhoon	0.7	0.2	0.8	1.1	55.8	1.1	39.4		1.0												
F4	Aerodrome	1.5	0.5	0.7	0.8	17.1	0.7	14.8	3.1	0.7	1.3	4.0	2.4	5.7	2.6	8.0	2.1	9.9	1.3	17.7	2.7	2.7
	Gilmore (TLE)	0.6		2.7	0.8	28.6	1.1	10.6	1.1	5.2	0.5	4.5	14.8	5.6	17.9	6.1						
	Gneiss	1.0	0.5	1.2	1.5	48.4	0.4	29.3	0.6	0.5	0.5	1.3	1.4	2.3	1.6	2.2	0.8	2.6	0.4	1.7	1.1	0.9
	Typhoon	1.1	0.2	1.3	0.3	7.7	0.2	3.5	2.6	0.6	4.0	7.6	5.4	11.6	6.1	15.5	4.8	15.9	1.6	6.2	0.8	3.0
F5	Aerodrome	4.5	4.2	3.1	4.4	38.8	0.8	19.5				2.4	4.7	3.4	6.1	1.4		2.9		1.6	2.3	
	Gilmore (TLE)	0.6		2.7	0.8	28.6	1.1	10.6	1.1	5.2	0.5	4.5	14.8	5.6	17.9	6.1						
	Gneiss	0.9	0.1	1.6	0.5	11.3	0.5	7.6	0.8	3.4	3.1	10.1	5.2	16.5	4.8	16.5	3.1	7.9	1.4	4.0	0.7	
	Typhoon	1.6	0.3	5.2	2.0	63.1	1.1	10.4		3.4	1.1	5.7	1.6									

Alcohols

Fraction	Sample	C14	C15	C16	C17	C18	C19	C20	C21	C22	C23	C24	C25	C26	C27	C28	C29	C30	C31	C32
F4	Aerodrome			0.8	0.1	1.8	27.3	2.4	2.2	5.4	2.1	9.8	2.3	13.6	2.4	18.0	1.5	7.1	1.2	2.1
	Gilmore (TLE)						0.4	1.4	0.7	7.3	2.0	7.9	2.8	20.1	4.1	28.0	3.4	15.0	2.9	4.1
	Gneiss		2.2	2.3	0.3	2.1	7.6	3.5	1.3	8.0	1.9	12.2	2.1	23.7	1.3	21.4	0.9	7.8	0.4	1.0
	Typhoon			1.1	0.2	1.2	2.5	5.9	3.5	11.1	3.0	11.0	2.8	17.7	2.3	18.1	1.7	15.0	0.5	2.5
F5	Aerodrome	1.2		1.8	1.8	18.6	3.8	3.4	2.8	6.0	2.6	9.8	2.0	11.5	5.1	15.5	9.3	1.6	3.2	
	Gilmore (TLE)						0.4	1.4	0.7	7.3	2.0	7.9	2.8	20.1	4.1	28.0	3.4	15.0	2.9	4.1
	Gneiss			0.8		4.7	4.5	6.4	1.2	7.3	1.8	11.6	2.1	23.4	6.6	20.1	7.4			
	Typhoon	5.3				6.2		13.9	4.7	17.0	3.3	8.9	11.7	4.8		5.3			19.1	

Sterols

Fraction	Sample	C27	C28	C29:2	C29:1
F4	Aerodrome	9.9	8.9	9.7	71.6
	Gilmore (TLE)				
	Gneiss	14.0	11.4	19.6	55.0
	Typhoon	16.4	9.4	17.6	56.6

Darker shading indicates higher abundances.

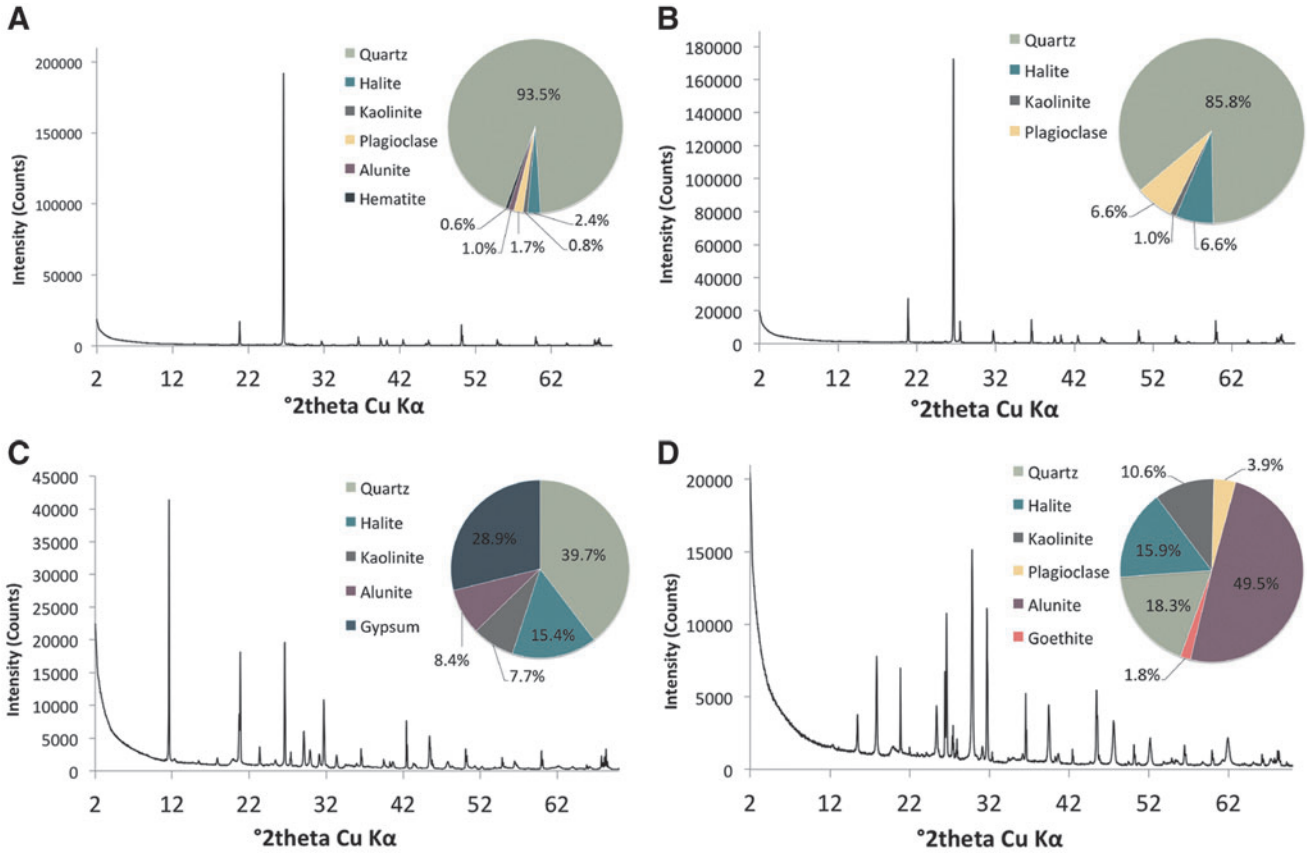

FIG. 2. Random powder XRD patterns and quantitative mineralogy for the mudflat/sandflat samples collected at **(A)** Aerodrome, **(B)** Typhoon, **(C)** Gilmore, and **(D)** Gneiss. XRD, X-ray diffraction.

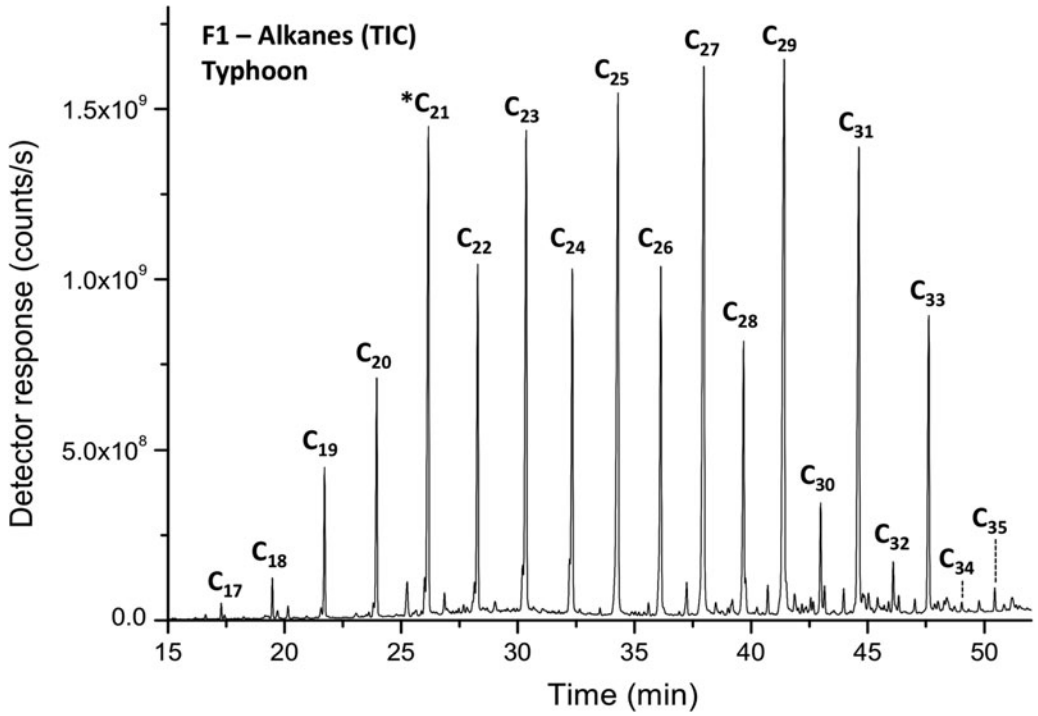

FIG. 3. A representative GC-MS chromatogram showing the detection of an odd-over-even carbon number preference in C_{17}–C_{35} alkanes in Typhoon Lake, a pattern indicative of terriginous plant material (Nonpolar Fraction F1). *Heneicosane (C_{21}) was added as an internal standard. GC-MS, gas chromatography-mass spectrometry; TIC, total ion current.

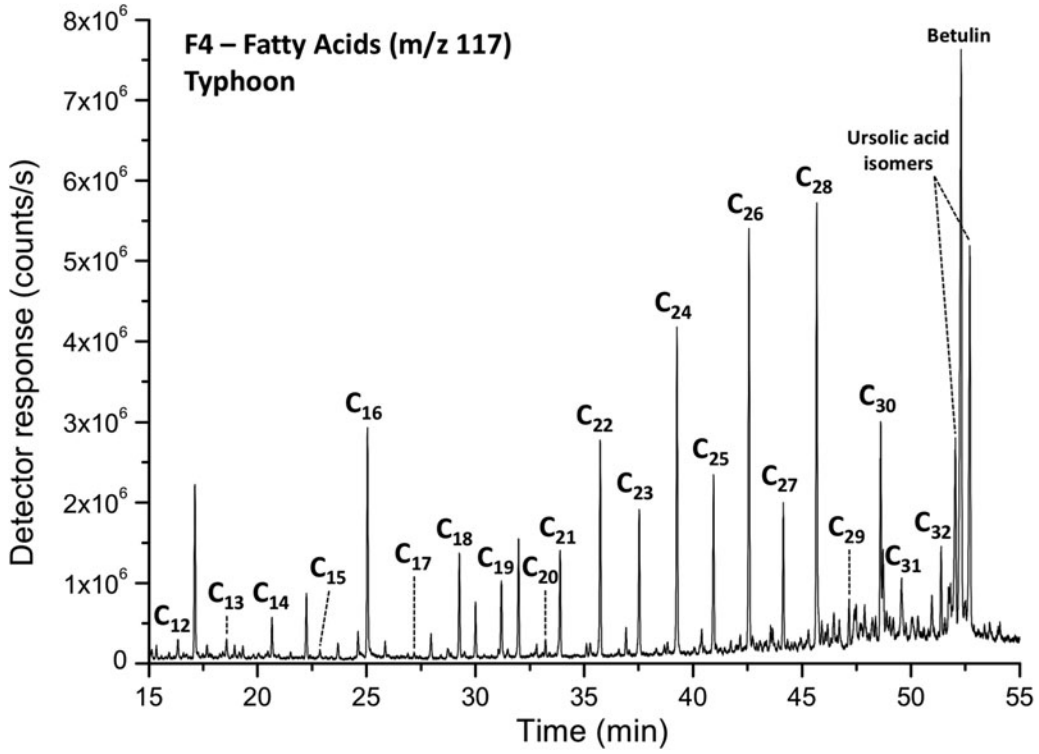

FIG. 4. A representative GC-MS chromatogram showing the detection of predominantly even carbon number fatty acids, as well as ursolic acid isomers and betulin, in Typhoon Lake (Polar Fraction F4). The shorter chain (*i.e.*, C_{16} and C_{18}) fatty acids shown are likely microbial in origin.

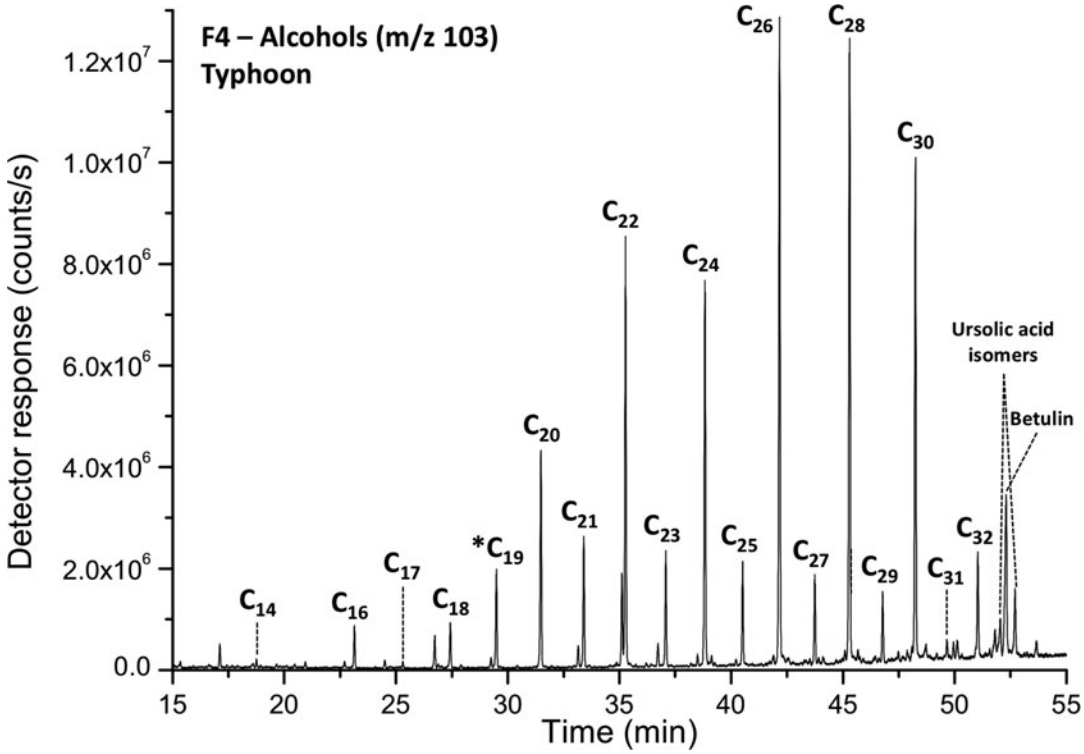

FIG. 5. A representative GC-MS chromatogram showing a predominantly even carbon number alcohols, as well as ursolic acid isomers and betulin, in Typhoon Lake (Polar Fraction F4). *1-Nonadecanol (C_{19}) was used as an internal standard.

times and fragmentation patterns, we also uncovered likely pentacyclic triterpenoids in some of the sampled sites, possibly bacterial hopanes or oleanane-type compounds.

5. Discussion

On Earth, organics are often sequestered in tandem with phyllosilicate minerals, such as smectites and associated noncrystalline iron and aluminum oxides/hydroxides (Wattel-Koekkoek *et al.*, 2003). Micrometer-size phyllosilicate minerals dominate the organic matter stabilization literature, in large part because these minerals have relatively large surfaces areas and typically carry a substantial charge, allowing them to chemically stabilize organic matter (Keil and Mayer, 2014). These observations suggest that terrain-dominated phyllosilicates are the best targets for lipid biomarker recovery; thus, sites with analogous phyllosilicate deposits on Mars, such as Jezero Crater, have been targeted for future exploration (Ehlmann *et al.*, 2013). The question remains as to whether phyllosilicates found in association with other mineral groups, such as the sulfate and iron oxide-bearing phyllosilicates of the Upper Murray unit at Gale crater (Rampe *et al.*, 2017), would also be worth targeting for sample return.

Our study is among the first to investigate the biomarker potential of mixtures of sulfates, iron oxides, and phyllosilicates in a highly acidic terrestrial Mars analogue. We found a strong odd over even carbon number predominance in long-chain *n*-alkanes (carbon preference index, or CPI, ranged from 3.6 to 5.7), indicating a terrigenous origin, probably in the primary form of cuticular waxes (Eglinton and Hamilton, 1967). These have also been shown to be carried in eolian dust (Simoneit, 1977; Gagosian *et al.*, 1987).

We also found a predominance of even numbered carbon compounds in the distributions of fatty acids and odd numbered compounds in the *n*-alcohols. Although even-over-odd carbon chain length preferences occur in short-chain fatty acids derived from microbial cellular processes (Volkman, 2006), even-over-odd long-chain fatty acids (>C20) are typically indicative of waxes and terrigenous plant inputs (Eglinton and Hamilton, 1967; Williams *et al.*, 2019). Although an algal origin of the long-chain fatty acids does remain a possibility, other signs of algae, such as higher levels of unsaturated fatty acids, would be expected (Volkman *et al.*, 1998). The predominance of C_{29} sterols over C_{27} and C_{28} sterols again suggests a land plant source (Huang and Meinscheim, 1979), and ursolic acid derivatives and betulin are indicative of higher plant leaf waxes (Jäger *et al.*, 2007).

The overall assemblage of saturated alkanes, alcohols, fatty acids, and sterols we recovered strongly point to the overprinting of plant debris, likely originating from the low-diversity eucalypt forests that exist on the Yilgarn Craton (Yates *et al.*, 2000), though low abundances of microbial lipids were also detected. We surmise that the amount of plant biomass simply overshadowed the traces of microbial biomass in the sediment, as diverse microbial communities have been observed within lake water and mud/sandflat sediment as part of genomic studies (Mormile *et al.*, 2009; Johnson *et al.*, 2015; Zaikova *et al.*, 2018). It is possible that there is a preservational bias for plant material in this system (perhaps sequestered in such a way that is more conducive to preservation) or simply for larger molecules (plant terpenoids, potential hopanes); however, easily hydrolyzed shorter chain fatty acids (*e.g.*, C_{16}, and C_{18}, likely associated with microbial communities) were also observed. It is interesting to note that although similar trends were found in terms of biomarker recovery as part of the 2005 pilot study (Johnson, 2008), there were noticeably fewer short-chain fatty acids recovered in this 2018 investigation. This may be due to seasonal fluctuation in the active microbial community, as the 2018 samples were collected in the Austral winter, whereas the 2005 samples were collected in the Austral summer when evapoconcentration and desiccation are most likely to occur. Although microbes may be present as part of an active subsurface microbial community, the plant lipids (very long chain alkanes, plant terpenoids, etc.) are certainly from dead organisms—washed into the lake basins at some point in the past. This suggests that structural biomarkers not only associated with extant biology are preserved through at least the early stages of diagenesis in the biosedimentary system represented by these lakes (Table 2).

Interestingly, we observed the highest levels of organic carbon associated with sulfate-bearing samples (Table 1). Substantial quantities of alunite (8.4 wt.%) and gypsum (28.9 wt.%) were found in the crystalline phase of our XRD data in the sediment of Lake Gilmore, which had the highest organic carbon content. The sediment of Lake Gneiss, which had the second highest organic carbon content, also had a significant sulfate-bearing component, with 49.5 wt.% alunite in the crystalline phase of our XRD data. These sulfate-rich lakes had the largest pH range difference among the lakes that we sampled (2.6–5.8 for Lake Gilmore, 1.4–3.7 for Lake Gneiss), suggesting that pH alone may not be a straightforward indicator of preservation. Some level of microbial activity may also be associated with the precipitation of acid salt lake sulfates (Johnson *et al.*, 2015), even though our results strongly suggest that plants are the dominant source of the organics recovered. We found the lowest organic carbon content, as well as the only below-detection levels of nitrogen, in Lake Aerodrome, where the sediments bore no sulfate-bearing minerals and were instead dominated by quartz.

Although there have been a few systematic investigations of the preservation potential of sulfate minerals on Earth, organics—including amino acids and their amine degradation products—have also been detected in Mars analog sulfate mineral matrices, including gypsum from the Anza-Borrego Desert, California, gypsum from the Haughton impact crater, Canada, and gypsum, anhydrite, and jarosite samples from Panoche Valley, California (Aubrey *et al.*, 2006), as well as ferric sulfate-rich streams in St. Oswald's Bay (Tan *et al.*, 2018) and acid saline lake gypsum from northern Chile (Benison and Karmanocky, 2014). Magnesium sulfates have also been shown to protect organics trapped inside the crystal lattice or present in fluid inclusions from oxidation induced by the decomposition of perchlorates, powerful oxidants present on the martian surface (François *et al.*, 2016).

Our results build on other recent findings that suggest that organics could be found in mineralogically diverse sediments on Mars, including those with jarosite group minerals (alunite, jarosite). It is possible that the presence of acid sulfate minerals alongside smectites and other phyllosilicates gave rise to habitable environments where

microbial activity was concentrated at redox interfaces, in the past or even today in the planet's subsurface. For example, a recent study of mudstones and sandstones in the Painted Desert of Arizona also revealed far higher concentrations of amino acids, in addition to carboxylic and dicarboxylic acids, alcohols, aliphatics, and other complex molecules, in the presence of clay minerals and jarosite together compared with the presence of clay minerals alone (Noe Dobrea *et al.*, 2016).

The processes affecting the preservation of organics in later stages of diagenesis, however, require additional investigation, and we have only investigated the very earliest stages of diagenesis as part of this study. There are very few examples of these types of depositional systems on Earth, but the ancient acid ephemeral saline lakes of the Permian Opeche Shale of the Williston Basin, North Dakota, provide one such opportunity (Benison *et al.*, 1998; Benison and Goldstein, 2002). Here, the oxidation of sulfide minerals along with other acidification processes, which may have been mediated by a combination of climate, rock-water interactions, and microbes, gave rise to extremely acidic waters (pH <1) in tectonically stable, closed-drainage basins (Benison and Bowen, 2015). These ancient sites precipitated evaporite minerals in an arid climate characterized by abundant, carbonate-poor red siliciclastics, much like lithified strata that have been observed on Mars at Gale crater. The discovery of lipid biomarkers in places such as the Permian Opeche Shale would further bolster the search for remnant organic matter on Mars.

Cosmic rays, UV irradiation, peroxides, and a multitude of nonaqueous chemical oxidations over very long timescales are critical challenges to the recovery of martian biomarkers (Summons *et al.*, 2008), and it is likely that deep subsurface samples from ancient acid saline playa lakes would be better targets for biomarker preservation on Mars than the shallow subsurface samples we analyzed here.

Although hyperaridity is a major challenge to microbial survival on Earth, the hyperaridity of the martian surface, which is 100–1000 times drier than the driest regions on Earth, may facilitate the preservation of lipids generated during environmentally favorable periods (Wilhelm *et al.*, 2017). There is extensive evidence that aqueous conditions were widespread on Mars in its ancient past; so if microbial life did arise on Mars before the desertification of the planet, biomarkers may still be preserved in the geological record.

6. Conclusion

Our investigation of the types of biomarkers recoverable within the naturally occurring acid salt lakes in the vicinity of Norseman, Western Australia—a terrestrial analogue with striking mineralogical and sedimentary similarities to Mars—has revealed the vestiges of several plant biomolecules alongside trace microbial lipids. The resilience of lipids from dead organic material in the saline sediments represented by these lakes lends support to the idea that sulfates, in tandem with phyllosilicates and iron oxides, may be a viable target for preserved biomarkers on Mars, and it motivates investigations of organic preservation in acidic saline pans that have been preserved in our planet's deep geological record.

Acknowledgments

The authors would like to thank Angus Turner for assistance in their initial survey of the area and Roger Summons for insightful advice on the article.

Author Disclosure Statement

No competing financial interests exist.

Funding Information

The authors would like to acknowledge the support of the William F. Milton Fund and a Georgetown University Main Campus Research Grant.

References

Aerts, J., Spanning, R.V., Flahaut, J., Molenaar, D., Bland, P., Ehrenfreund, P., and Martins, Z. (2019) Microbial communities from four mildly acidic ephemeral salt lakes in the Yilgarn Craton (Australia)–terrestrial analogues to ancient Mars. *Front Microbiol* 10:779.

Aubrey, A., Cleaves, H.J., Chalmers, J.H., Skelley, A.M., Mathies, R.A., Grunthaner, F.J., Ehrenfreund, P., and Bada, J.L. (2006) Sulfate minerals and organic compounds on Mars. *Geology* 34:357–360.

Benison, K.C. and Bowen, B.B. (2006) Acid saline lake systems give clues about past environments and the search for life on Mars. *Icarus* 183:225–229.

Benison, K.C. and Bowen, B.B. (2015) The evolution of end-member continental waters: the origin of acidity in southern Western Australia. *GSA Today* 25:4–10.

Benison, K.C. and Goldstein, R.H. (2002) Recognizing acid lakes and groundwaters in the rock record. Sediment Geol 151:177–185.

Benison, K.C. and Karmanocky, F.J. (2014) Could microorganisms be preserved in Mars gypsum? Insights from terrestrial examples. Geology 42:615–618.

Benison, K.C. and LaClair, D.A. (2003) Modern and ancient extremely acid saline deposits: terrestrial analogs for martian environments? Astrobiology 3:609–618.

Benison, K.C., Goldstein, R.H., Wopenka, B., Burruss, R.C., and Pasteris, J.D. (1998) Extremely acid Permian lakes and ground waters in North America. Nature 392:911–914.

Benison, K.C., Bowen, B.B., Oboh-Ikuenobe, F.E., Jagniecki, E.A., LaClair, D.A., Story, S.L., Mormile, M.R., and Hong, B.-Y. (2007) Sedimentology of acid saline lakes in southern Western Australia: newly described processes and products of an extreme environment. *J Sediment Res* 77:366–388.

Benison, K.C., Jagniecki, E.A., Edwards, T.B., Mormile, M.R., and Storrie-Lombardi, M.C. (2008) ''Hairy blobs'': microbial suspects preserved in modern and ancient extremely acid lake evaporites. *Astrobiology* 8:807–821.

Bligh, E.G. and Dyer, W.J. (1959) A rapid method of total lipid extraction and purification. *Can J Biochem Physiol* 37: 911–917.

Bowen, B.B. and Benison, K.C. (2009) Geochemical characteristics of naturally acid and alkaline saline lakes in southern Western Australia. *Appl Geochem* 24:268–284.

Bowen, B.B., Benison, K.C., Oboh-Ikuenobe, F.E., Story, S., and Mormile, M.R. (2008) Active hematite concretion formation in modern acid saline lake sediments, Lake Brown, Western Australia. *Earth Planet Sci Lett* 288:52–63.

Bowen, B.B., Benison, K.C., and Story, S. (2012) Early diagenesis by modern acid brines in Western Australia and

implications for the history of sedimentary modification on Mars. In *SEPM Special Publication 102: Sedimentary Geology of Mars*, edited by J. Grotzinger and R. Milliken, Society for Sedimentary Geology, Tulsa, Oklahoma, pp 229–252.

Bowen, B.B., Story, S., Oboh-Ikuenobe, F.E., and Benison, K.C. (2013) Differences in regolith weathering history at an acid and neutral saline lake on the Archean Yilgarn Craton and implications for acid brine evolution: *Chem Geol* 356: 126–140.

Burns, R.G. (1987) Gossans on Mars: spectral features attributed to jarosite. *Lunar and Planetary Science Conference* 18: 141.

Catalano, J.G. (2013) Thermodynamic and mass balance constraints on iron-bearing phyllosilicate formation and alteration pathways on early Mars. *J Geophys Res Planets* 118: 2124–2136.

Cull, S., McGuire, P.C., Gross, C., Myers, J., and Shmorhun, N. (2014) A new type of jarosite deposit on Mars: evidence for past glaciation in Valles Marineris? *Geology* 42:959–962.

De Leeuw, J.W. and Largeau, C. (1993) A review of macromolecular organic compounds that comprise living organisms and their role in kerogen, coal, and petroleum formation. In *Organic Geochemistry*, edited by M.H. Engel and S.A. Macko, Springer, Boston, MA, pp 23–72.

Eglinton, G. and Hamilton, R.J. (1967) Leaf epicuticular waxes. *Science* 156:1322–1335.

Ehlmann, B.L., Berger, G., Mangold, N., Michalski, J.R., Catling, D.C., Ruff, S.W., Chassefière, E., Niles, P.B., Chevrier, V., and Poulet, F. (2013) Geochemical consequences of widespread clay mineral formation in Mars' ancient crust. *Space Sci Rev* 174:329–364.

Ehlmann, B.L., Swayze, G.A., Milliken, R.E., Mustard, J.F., Clark, R.N., Murchie, S.L., Breit, G.N., Wray, J.J., Gondet, B., and Poulet, F. (2016) Discovery of alunite in Cross crater, Terra Sirenum, Mars: evidence for acidic, sulfurous waters. *Am Mineral* 101:1527–1542.

François, P., Szopa, C., Buch, A., Coll, P., McAdam, A.C., Mahaffy, P.R., Freissinet, C., Glavin, D.P., Navarro-Gonzalez, R., and Cabane, M. (2016) Magnesium sulfate as a key mineral for the detection of organic molecules on Mars using pyrolysis. *J Geophys Res Planets* 121:61–74.

Gagosian, R.B., Peltzer, E.T., and Merrill, J.T. (1987) Long-range transport of terrestrially derived lipids in aerosols from the South Pacific. *Nature* 325:800–803.

Huang, W.-Y. and Meinschein, W.G. (1979) Sterols as ecological Indicators. *Geochim Cosmochim Acta* 43:739–745.

Jäger, S., Winkler, K., Pfüller, U., and Scheffler, A. (2007) Solubility studies of oleanolic acid and betulinic acid in aqueous solutions and plant extracts of Viscum album L. *Planta Med* 73:157–162.

Johnson, S.S. (2008) Mars in the Late Noachian: evolution of a habitable surface environment (Doctoral dissertation, Massachusetts Institute of Technology). Available online at https://dspace.mit.edu/handle/1721.1/45605

Johnson, S.S., Chevrette, M.G., Ehlmann, B.L., and Benison, K.C. (2015) Insights from the metagenome of an acid salt lake: the role of biology in an extreme depositional environment. *PLoS One* 10:e0122869.

Keil R.G. and Mayer L.M. (2014) Mineral matrices and organic matter. In *Treatise on Geochemistry, Second Edition*, vol. 12, edited by H.D. Holland and K.K. Turekian. Elsevier, Oxford, UK, pp 337–359.

Klein, C. (2005) Some Precambrian banded iron-formations (BIFs) from around the world: their age, geologic setting, mineralogy, metamorphism, geochemistry, and origins. *Am Mineral* 90:1473–1499.

Klingelhöfer, G., Morris, R.V., Bernhardt, B., Schröder, C., Rodionov, D.S., De Souza, P., Yen, A., Gellert, R., Evlanov, E., and Zubkov, B. (2004) Jarosite and hematite at Meridiani Planum from Opportunity's Mössbauer spectrometer. *Science* 306:1740–1745.

Léveillé, R., Oehler, D., Fairen, A., Clark, B., Niles, P., and Blank, J. (2015) Jarosite in Gale crater, Mars: the importance of temporal and spatial variability and implications for habitability. *Astrobiology Science Conference*, 7307.

McCollom, T.M. and Seewald, J.S. (2007) Abiotic synthesis of organic compounds in deep-sea hydrothermal environments. *Chem Rev* 107:382–401.

Mormile, M.R., Hong, B.-Y., and Benison, K.C. (2009) Molecular analysis of the microbial communities of Mars analog lakes in Western Australia. *Astrobiology* 9:919–930.

Noe Dobrea, E., McAdam, A., Freissinet, C., Franz, H., Belmahdi, I., Hamersley, M., Stoker, C., Parker, W., Glavin, D., and Calef, F. (2016) Preservation of organics at the painted desert: Lessons for MSL and beyond. *LPI Contributions*, 1912.

Nordstrom, D.K. (1982) The effect of sulfate on aluminum concentrations in natural waters: some stability relations in the system Al2O3-SO3-H2O at 298 K. *Geochim Cosmochim Acta* 46:681–692.

Ohmoto, H. and Lasaga, A.C. (1982) Kinetics of reactions between aqueous sulfates and sulfides in hydrothermal systems. *Geochim Cosmochim Acta* 46:1727–1745.

Pentrák, M., Madejová, J., Andrejkovičová, S., Uhlík, P., and Komadel, P. (2012) Stability of kaolin sand from the Vyšný Petrovec deposit (south Slovakia) in an acid environment. *Geol Carpath* 63. doi: 10.2478/v10096-012-0039-x.

Peters, K.E., Walters, C.C., and Moldowan, J.M. (2007) *The Biomarker Guide: Volume 1, Biomarkers and Isotopes in the Environment and Human History.* Cambridge University Press, Cambridge, U.K.

Rampe, E., Ming, D., Grotzinger, J., Morris, R., Blake, D., Vaniman, D., Bristow, T., Morrison, S., Yen, A., and Chipera, S. (2017) Mineral trends in early Hesperian lacustrine mudstone at Gale crater, Mars. *Lunar and Planetary Science Conference* 48: 2821.

Simoneit, B.R. (1977) Biogenic lipids in particulates from the lower atmosphere over the eastern Atlantic. *Nature* 267: 682–685.

Simoneit, B.R., Summons, R., and Jahnke, L. (1998) Biomarkers as tracers for life on early Earth and Mars. *Origins Life Evol Biosph* 28:475–483.

Story, S., Bowen, B.B., Benison, K.C., and Schulze, D.G. (2010) Authigenic phyllosilicates in modern acid saline lake sediments and implications for Mars. *J Geophys Res Planets* 115:E12012.

Stumm, W. and Morgan, J.J. (1996) *Aquatic chemistry: chemical equilibria and rates in natural waters* (3rd Ed). John Wiley & Sons, New York.

Stumm, W. and Morgan, J.J. (2012) *Aquatic Chemistry: Chemical Equilibria and Rates in Natural Waters*. John Wiley & Sons, New York.

Summons, R.E. and Walter, M.R. (1990) Molecular fossils and microfossils of prokaryotes and protists from Proterozoic sediments. Am J Sci 290A:212–244.

Summons, R.E., Albrecht, P., McDonald, G., and Moldowan, J.M. (2008) Molecular biosignatures. In *Strategies of Life Detection*. Springer, Boston, MA, pp 133–159.

Sumner, D.Y. (2004) Poor preservation potential of organics in Meridiani Planum hematite-bearing sedimentary rocks. *J Geophys Res Planets* 109:E12007.

Tan, J., Lewis, J.M.T., and Sephton, M.A. (2018) The fate of lipid biosignatures in a Mars-analogue sulfur stream. *Nat Sci Rep* 8:7586.

Tosca, N.J., McLennan, S.M., Clark, B.C., Grotzinger, J., Hurowitz, J.A., Knoll, A.H., Schröder, C., and Squyres, S.W. (2005) Geochemical modeling of evaporation processes on Mars: insight from the sedimentary record at Meridiani Planum. *Earth Planet Sci Lett* 240:122–148.

Volkman, J. (2006) Lipid biomarkers for marine organic matter. In *Marine Organic Matter: Biomarkers, Isotopes and DNA*, edited by J. Volkman. Springer-Verlag, Heidelberg, Berlin, pp 27–70.

Volkman, J.K., Barrett, S.M., Blackburn, S.I., Mansour, M.P., Sikes, E.L., and Gelin, F. (1998) Microalgal biomarkers: a review of recent research developments. *Org Geochem* 29: 1163–1179.

Wattel-Koekkoek, E., Buurman, P., Van Der Plicht, J., Wattel, E., and Van Breemen, N. (2003) Mean residence time of soil organic matter associated with kaolinite and smectite. *Eur J Soil Sci* 54:269–278.

White, D.C. (1983) Analysis of microorganisms in terms of quantity and activity in natural environments. In *Microbes in Their Natural Environments,* edited by J.H. Slater, R. Whittenbury, and J.W.T. Wimpenny. Cambridge University Press, Cambridge, UK, pp 37–66.

Wilhelm, M.B., Davila, A.F., Eigenbrode, J.L., Parenteau, M.N., Jahnke, L.L., Liu, X., Summons, R.E., Wray, J.J., Stamos, B.N., O'Reilly, S.S., and Williams, A.J. (2017) Xeropreservation of functionalized lipid biomarkers in hyperarid soils in the Atacama Desert. *Org Geochem* 103:97–104.

Wilhelm, M.B., Davila, A.F., Parenteau, M.N., Jahnke, L.L., Abate, M., Cooper, G., Kelly, E.T., Garcıa, V.P., Villadangos, M.G., Blanco, Y., Glass, B., Wray, J.J., Eigenbrode, J.L., Summons, R.E., and Warren-Rhodes, K. (2018) Constraints on the metabolic activity of microorganisms in Atacama surface soils inferred from refractory biomarkers: Implications for martian habitability and biomarker detection. *Astrobiology* 18:955–966.

Williams, A.J., Eigenbrode, J., Floyd, M., Wilhelm, M.B., O'Reilly, S., Johnson, S.S., Craft, K.L., Knudson, C.A., Andrejkovičová, S., Lewis, J.M.T., Buch, A., Glavin, D.P., Freissinet, C., Williams, R.H., Szopa, C., Millan, M., Summons, R.E., McAdam, A., Benison, K., Navarro-González, R., Malespin, C., and Mahaffy, P.R. (2019) Recovery of fatty acids from mineralogic Mars analogs by TMAH thermochemolysis for the sample analysis at Mars wet chemistry experiment on the curiosity Rover. *Astrobiology* 19: 522–546.

Yates, C.J., Hobbs, R.J., and True, D.T. (2000) The distribution and status of eucalypt woodlands in Western Australia. In *Temperate eucalypt woodlands in Australia: biology, conservation, management and restoration.* Edited by R.J. Hobbs and C.J. Yates, Surrey Beatty & Sons, Chipping Norton, New South Wales, Australia, pp 86–106.

Zaikova, E., Benison, K.C., Mormile, M.R., and Johnson, S.S. (2018) Microbial communities and their predicted metabolic functions in a desiccating acid salt lake. *Extremophiles* 22:367–379.

Zolotov, M.Y. and Mironenko, M.V. (2016) Chemical models for martian weathering profiles: insights into formation of layered phyllosilicate and sulfate deposits. *Icarus* 275: 203–220.

Address correspondence to:
Sarah Stewart Johnson
Department of Biology
Georgetown University
Regents 511
37th & O Streets, NW
Washington, DC 20057

E-mail: sarah.johnson@georgetown.edu

Submitted 29 December 2017
Accepted 13 August 2019

Abbreviations Used

BSTFA = bis(trimethylsilyl)trifluoroacetamide
GC-MS = gas chromatography-mass spectrometry
PTV = programmed-temperature vaporization
RIR = relative intensity ratio
TDS = total dissolved solids
TMS = Trimethylsilyl
XRD = X-ray diffraction